Journal of Solid State Chemistry 183 (2010) 1555–1560

Contents lists available at ScienceDirect

Journal of Solid State Chemistry

journal homepage: www.elsevier.com/locate/jssc

The influence of silica matrix on the crystal structure and high frequency performance of cobalt nanoparticles

Xuegang Lu *, Gongying Liang, Qianjin Sun, Caihua Yang

MOE Key Laboratory for Non-equilibrium Synthesis and Modulation of Condensed Matter, School of Science, Xi'an Jiaotong University, Xi'an 710049, China

ARTICLE INFO

Article history:
Received 21 January 2010
Received in revised form
19 April 2010
Accepted 21 April 2010
Available online 24 April 2010

Keywords:
Magnetic materials
Nanocomposite
Crystal structure
Permeability spectra

ABSTRACT

Cobalt–SiO_2 nanocomposites were successfully synthesized by chemical precipitation combined H_2 reduction method. The influence of SiO_2 matrix on the crystal structure and high frequency magnetic properties of cobalt nanoparticles was investigated. Amorphous SiO_2 layer, which is adhered to Co particle surface through Si–O–Co bonds, inhibits the growth of the nanoparticles and stabilizes the face-centered-cubic (FCC) structured Co. The FCC-cobalt/SiO_2 nanocomposites exhibit soft magnetic behavior with saturation magnetization (M_s) about 125 emu/g and coercivity (H_c) smaller than 100 Oe. The permeability spectra of Co/SiO_2 nanocomposites depend on the SiO_2 contents. When the SiO_2 content is greater than 8 wt%, the permeability spectra demonstrate notable high frequency characteristic, in which the real part μ' of the permeability is almost independent of frequency and the imaginary part μ'' remains extremely low in high frequency range.

1. Introduction

The rapid developments of wireless communication devices have required miniature magnetic components, such as inductor and transformer, to be operated at high frequency [1–4]. Suitability requirements of magnetic materials for high-frequency applications are large saturation magnetization (M_s), high permeability μ' and low energy losses [5,6]. None of the existing bulk magnetic alloys satisfy these requirements because of large eddy-current loss induced by low resistivity. Mn–Zn, Ni–Zn or Co_2Z ferrites have an intrinsic disadvantage of small saturation magnetization M_s. The high-frequency performance of these ferrite cores is limited by Snoek's law [7,8]. Magnetic nanocomposites, in which ferromagnetic nanoparticles are dispersed in an insulating matrix (e.g., silica, alumina, polymer, or ferrites), have attracted considerable attention due to their potential uses as high-density magnetic storage media [9], microwave absorbing and shielding materials [10,11] and novel high-frequency soft magnetic materials [5,11,12]. The resistivity of metal/insulator nanocomposites can be dramatically increased as compared to conventional metallic alloys, leading to significantly reduced eddy-current loss. Large saturation magnetization (M_s), which can be obtained by adjusting the metal/insulator ratio, helps to improve the Snoek limit. Keeping the particle size in nanometer scale can lower the energy loss caused by domain wall resonance. Meanwhile, the exchange coupling between neighboring magnetic nanoparticles can overcome the anisotropy and demagnetizing effects, resulting in much better soft magnetic properties than conventional materials [13].

Among metal/insulator magnetic composites, cobalt/SiO_2 nanocomposites have attracted great interests from both theoretical and technological points of view due to their particular structural, magnetic and other physicochemical properties [14]. Pure cobalt in bulk form has hexagonal-closed-packed (HCP) crystal structure at ambient temperature and goes through martensitic transformation to FCC structure at 420 °C [15–17]. Interestingly, FCC structure of Co can be retained at room temperature if the particle size is controlled in nanometer scale [16–18]. FCC-Co is necessary for soft magnetic materials because of its small anisotropy fields compared to HCP-Co. How to obtain FCC-Co nanoparticles (NPs) is a key problem to manufacture Co-based soft magnetic materials. Imbedding Co NPs into amorphous SiO_2 can effectively improve the electrical resistivity of the materials and suppress eddy-current losses in high frequency operations. SiO_2 matrix also hinders growth, aggregation and oxidation of Co NPs during the formation of nanoparticles. And most importantly, SiO_2 matrix on Co particle surface can stabilize the FCC structure of Co particles.

In this paper, we report a facile method to prepare FCC-Co NPs imbedded into amorphous SiO_2 matrix. The influence of SiO_2 matrix on the crystal structure and high frequency magnetic properties of Co NPs was investigated.

2. Experimental

All reagents are of analytical grade and used as obtained without further purification. The typical preparation procedure of

* Corresponding author. Fax: +86 29 87662630.
E-mail address: xglu@mail.xjtu.edu.cn (X. Lu).

0022-4596/$ - see front matter © 2010 Elsevier Inc. All rights reserved.
doi:10.1016/j.jssc.2010.04.031

cobalt/SiO_2 nanocomposites is as follows [19]: 100 ml $CoCl_2$ solution (0.4 mol/l) and 40 ml sodium hydroxide (NaOH) solution (1 mol/l) were simultaneously added to 200 ml deionized water (70 °C) with rapid stirring. A pink precipitation formed instantly. The pH value of the solution was kept in the range $12 \leq pH \leq 14$ by adjusting the amount of NaOH. 2 ml surfactant (polyethylene glycol) was added to the suspension to prevent the particles from aggregating. After 10 min, sodium silicate ($Na_2SiO_3 \cdot 9H_2O$) solution was injected into the suspension under vigorous stirring, controlling the molar ratio of Co^{2+}:SiO_2 at 97:3, 95:5, 92:8, 88:12, 84:16 and 80:20, respectively. During this period, the pH value was kept in the range $7 \leq pH \leq 9$ for completing the hydrolyzation of sodium silicate and the precipitation of silicate. The suspension was repeatedly washed, filtered for several times and dried at 100 °C in air. The dried powders were then annealed in an electric heated quartz furnace under a continuous hydrogen flow.

The phase structure of the cobalt/SiO_2 nanocomposites was determined by powder X-ray diffraction (XRD) analysis using Cu $K\alpha_1$ radiation. Morphology was analyzed using transmission electron microscopy (TEM). Micro-Raman spectroscopy was used to investigate the interaction between Co particle and silica coating. Magnetic properties were studied using a Lake Shore vibrating sample magnetometer (VSM) with a maximum applied magnetic field of 10,000 Oe. The composite particles were compacted into toroidal cores for the permeability measurement at the pressure 12 ton/cm^2. The toroidal size is φ3 mm in inside diameter, φ7 mm in outside diameter and 2 mm in height. Complex permeability spectra were measured in the range 1 MHz to 1 GHz with an RF impedance/material analyzer (Agilent4291B+16454A).

3. Results and discussion

Fig. 1 shows the XRD patterns of cobalt/SiO_2 nanocomposites with different SiO_2 contents. The samples were reduced by H_2 at 560 °C for 2 h. It can be seen that FCC-Co is observed in all of the samples. It is noteworthy that only FCC-Co is found when SiO_2 contents are 8 wt% and 12% (Fig. 1b and c), respectively. No peaks for CoO or HCP-Co are detected. But when the SiO_2 content is decreased to 5 wt% (Fig. 1a), a trace of HCP-Co can be observed. On the other hand, when the SiO_2 contents increase from 16 to 20 wt% (Fig. 1d and e), CoO appears and increases accordingly. No crystalline SiO_2 is detected in all the samples. As a result, we conclude that SiO_2 phase in the Co/SiO_2 nanocomposites is in amorphous state.

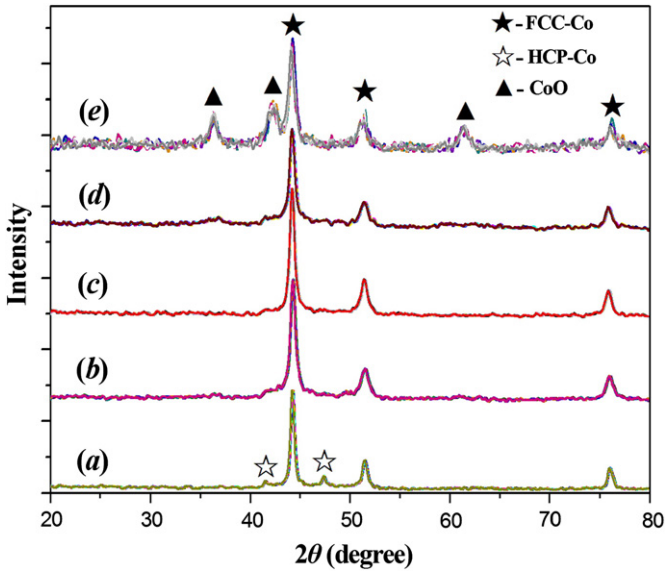

Fig. 1. XRD patterns of Co/SiO_2 nanocomposite powders synthesized by H_2 reduction at 560 °C for 2 h: (a) 5 wt% SiO_2, (b) 8 wt% SiO_2, (c) 12 wt% SiO_2, (d) 16 wt% SiO_2 and (e) 20 wt% SiO_2.

Fig. 2 shows TEM images, electron diffraction patterns and Raman spectra of the Co/SiO_2 nanocomposites prepared by H_2 reduction at 560 °C for 2 h. SiO_2 contents are 5 and 8 wt%, respectively. It can be seen that nearly spherical shaped Co NPs are imbedded in SiO_2. When SiO_2 content is 5 wt% the particle size of Co is in the range 30–80 nm. When SiO_2 content is increased to 8 wt%, the particle size can be retained in the range 20–30 nm. The electron diffraction patterns (Fig. 2c) exhibit the diffraction peaks from (1 1 1), (2 0 0) and (2 2 0) planes of FCC-Co, which further confirms the results of XRD patterns (Fig. 1b). Raman features peaking at 440, 805, 1065 and 1200 cm^{-1} are related to the silica network (Fig. 2d). The additional bands at 695 and 880 cm^{-1} are characteristic of the Si–O–Co bonds [20]. This indicates that Co NPs are encapsulated by SiO_2 through chemical bonds. The formation of SiO_2 layer on Co particles is illustrated in Scheme 1. In alkaline solution ($7 \leq pH \leq 9$), sodium silicate quickly hydrolyzes to form high active metasilicic acid ($Si(OH)_4$). Then condensation reaction of $Si(OH)_4$ will take place on the interface between $Co(OH)_2$ and $Si(OH)_4$ mediated by OH groups, which bonded to the $Co(OH)_2$ surface. This leads to the formation of Si–O–Co bonds and a SiO_2 layer. With further reaction, SiO_2 network forms around Co NPs.

It is well known that pure Co metal in bulk form has HCP crystal structure below allotropic transformation temperature of 420 °C and undergoes a martensitic transformation to FCC structure above 420 °C [15–17]. Different from the bulk form of Co, the FCC-Co structure can be retained even at room temperature when the particle size of Co is reduced into nanometer scale [18]. This is believed to be due to the lower surface energy density of FCC-Co NPs compared to that of HCP-Co [21]. Thermodynamic analysis shows there exists a critical particle size (r_c) for the structure transformation from FCC-Co to HCP-Co. Below r_c, Co can exist in stable FCC phase. Moreover, since the lattice volume $\boldsymbol{V}$ of FCC-Co and HCP-Co are 44.63 and 66.50 nm^{-3}, respectively, SiO_2 layer that adhered to Co NPs surface mediated by Si–O–Co bonds must append extra strain energy to Co NPs when FCC→HCP transformation takes place. This extra strain energy enlarges the critical particle size r_c. So Co NPs coated by SiO_2 behaves in a more stable manner in FCC structure than that without SiO_2. Previous studies have shown that Co NPs are stable only when the particle size is smaller than 20 nm [22]. In this paper, however, FCC-Co can be retained even when the particle size is as large as 60–80 nm. When SiO_2 content is lower than 5 wt%, Co NPs are apt to grow and some of them become large enough to exceed the critical size r_c. Hence, HCP-Co appears. With the increase of SiO_2 content, the growth of the nanoparticles is retarded and single FCC-Co phase is obtained. With the further increase of SiO_2 content, the reduction of CoO to Co becomes difficult and some of the CoO remains in the final composite.

Apart from SiO_2 content, the phase structure of as-prepared Co/SiO_2 nanocomposite is also determined by the reducing time and reducing temperature. It is reasonable that with the increase of reducing time, the particle size of Co should increase accordingly. If the particle size exceeds the critical size r_c, HCP-Co should appear. Fig. 3 shows the XRD patterns of Co/SiO_2 nanocomposites synthesized by H_2 reduction at 560 °C for different time t. It can be seen that when SiO_2 content is 3 wt% (Fig. 3a), merely 1 h reduction is adequate to convert CoO to Co completely. And at the same time, HCP-Co appears significantly. When SiO_2 contents increase to 16–20 wt% (Fig. 3c and d), the

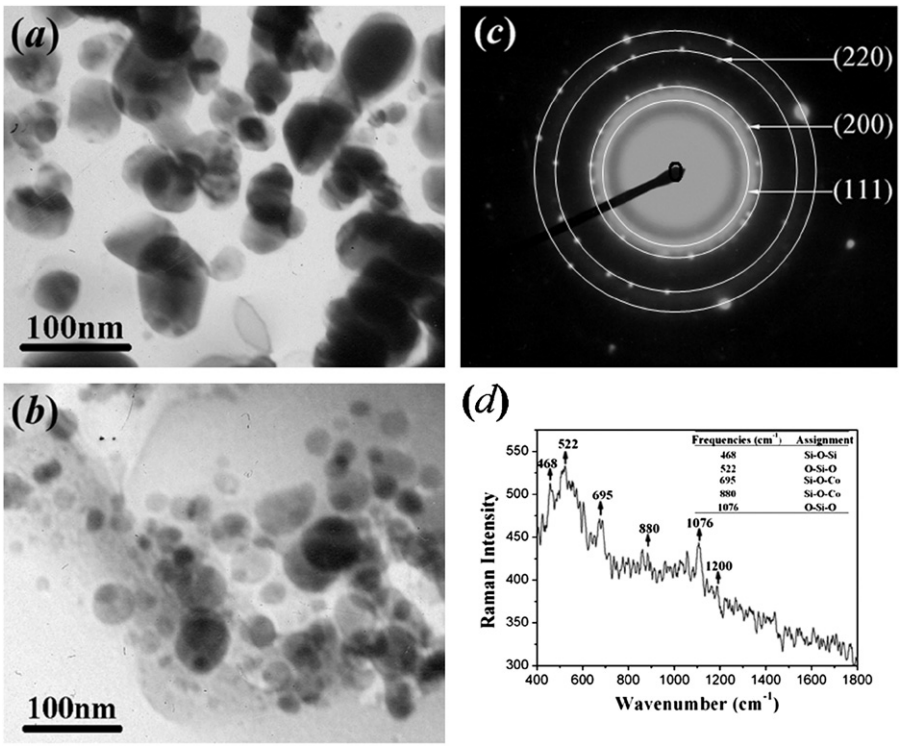

Fig. 2. Characterization of Co/SiO_2 nanocomposites synthesized by H_2 reduction at 560 °C for 2 h: TEM images of Co/SiO_2 nanocomposites with (a) 5 wt% SiO_2 and (b) 8 wt% SiO_2. (c) Electron diffraction patterns of Co/SiO_2 nanocomposites with 8 wt% SiO_2. (d) Raman spectra of the Co/SiO_2 nanocomposites with 8 wt% SiO_2.

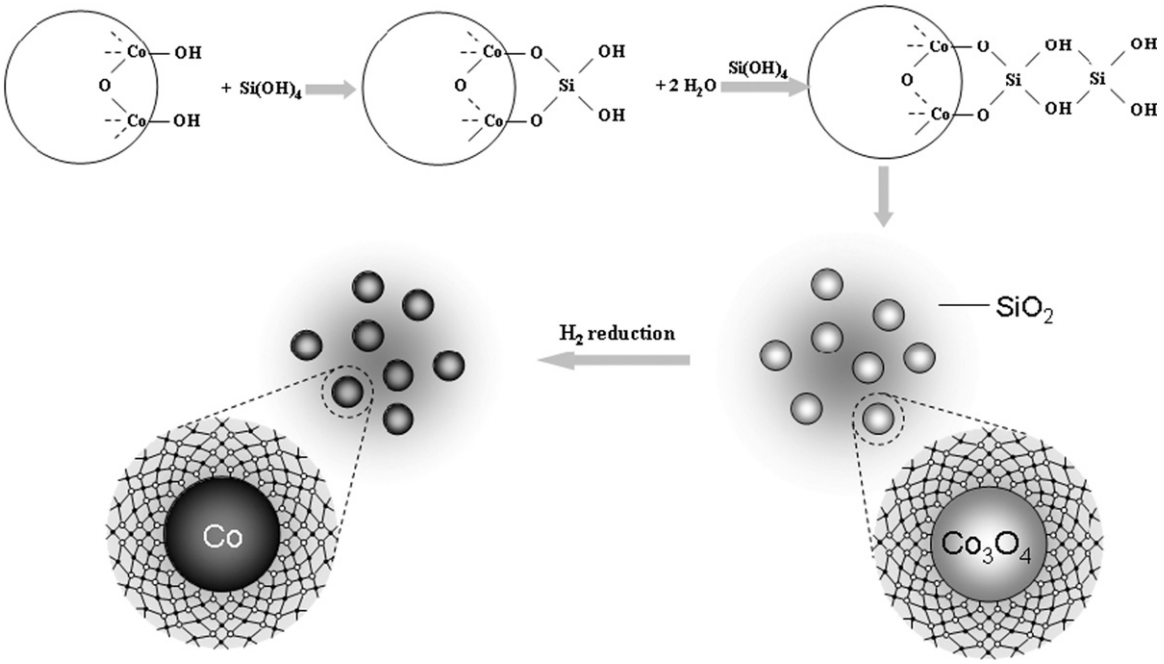

Scheme 1. Schematic diagram illustrating the formation of SiO_2 amorphous layer on Co particles.

reducing time must be extended accordingly so that CoO can be completely reduced to Co. Meanwhile, long time annealing leads to increase of particle size, so that HCP-Co begins to form. To obtain single FCC-Co, reduction time should be optimized according to the SiO_2 content.

Fig. 4 shows XRD patterns of $Co_8/(SiO_2)_{92}$ nanocomposites synthesized by H_2 reduction at different temperatures for 2 h. It can be seen that cobalt oxide is difficult to be completely reduced into Co metal phase when the reducing temperature is below 350 °C ($T \leq 350$ °C). With the increase of reducing temperature to 400 °C, only HCP-Co can be obtained and no FCC-Co is observed. When the reducing temperature is increased to 500–700 °C, single FCC-Co is obtained. With the further increase of the reducing temperature from 800 to 900 °C, some amount of HCP-Co begins to appear again. This reveals that single FCC-Co cannot be achieved if the reducing temperature is lower than the martensitic transformation temperature of 420 °C. In addition, high reducing temperatures (>800 °C) are likely to cause the

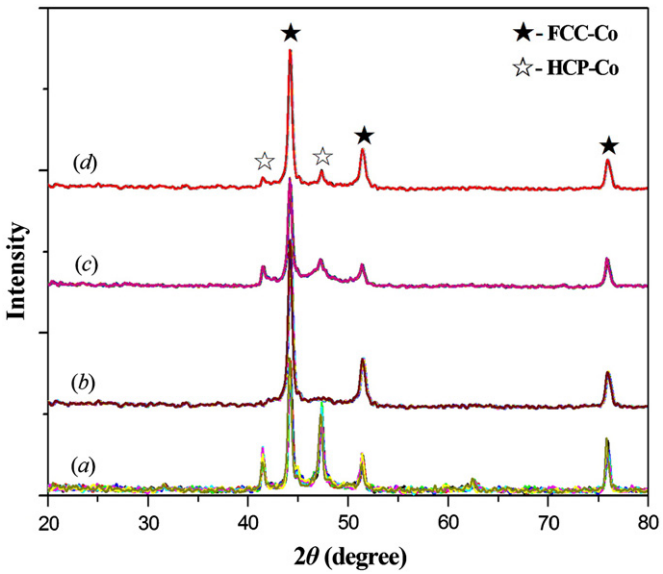

Fig. 3. XRD patterns of $Co_{1-x}/(SiO_2)_x$ nanocomposites synthesized by H_2 reduction at 560 °C for different time t: (a) $x=3$ wt%, $t=1$ h; (b) $x=8$ wt%, $t=2$ h; (c) $x=16$ wt%, $t=6$ h; (d) $x=20$ wt%, $t=16$ h.

growth of the nanoparticles so that HCP-Co forms. From this it can be estimated that to achieve FCC-Co NPs, the reducing temperature should not be lower than 420 °C and higher than 800 °C.

Fig. 5 shows the magnetic hysteresis loops for $Co_{92}/(SiO_2)_8$ nanocomposites synthesized by H_2 reduction at 400, 560 and 700 °C. It can be seen that the coercivity (H_c) of the nanocomposites decreases with the increase of reducing temperature. The coercivity (H_c) of the nanocomposites prepared at 560 °C ($H_c \approx 100$ Oe) and 700 °C ($H_c \approx 60$ Oe) are much smaller than that prepared at 400 °C (250 Oe). This can be attributed to the different anisotropy fields between FCC-Co and HCP-Co. Since the anisotropy fields for FCC-Co and HCP-Co are approximately 500 Oe and 10 kOe [23], respectively, the coercivity of the nanocomposites reduced at 560 and 700 °C (FCC-Co) should be smaller than that reduced at 400 °C (HCP-Co). The saturation magnetization (M_s) of the $Co_{92}/(SiO_2)_8$ NPs reduced at 560 °C is about 125 emu/g, which is 2–3 times larger than that of traditional ferrite. From the Snoek formula $(\mu_r-1)f_r=1/3\gamma M_s$, where γ is the gyromagnetic ratio, high M_s is favorable for high-frequency soft magnetic materials.

Fig. 6 shows the frequency dependence of the complex permeability for the cores made of Co/SiO_2 nanocomposites reduced at 560 °C for 2 h. When the SiO_2 content is 3 wt%, the real part of permeability μ' decreases rapidly with the increase of frequency at the lower frequency range. With further increase of SiO_2 content, the cut-off frequency moves to the high frequency range gradually. When the SiO_2 content is 8 wt%, a remarkable feature in which the real part μ' ($\mu' \approx 7$) of the permeability is almost independent of frequency (below 1 GHz) can be observed. This high frequency performance is believed to be due to the insulation provided by SiO_2 coating. For metallic magnetic materials, μ' decreases rapidly with the increase of frequency in the low frequency range due to the eddy currents arising from poor insulation between particles. But in Co/SiO_2 nanocomposites, SiO_2 insulation between particles drastically enhances the resistivity of the materials, consequently inhibiting eddy currents and pushes the cut-off frequency up to the high frequency range.

In conventional magnetic materials, the change of the magnetization vector is generally brought about by rotation of the magnetization or the domain wall displacement. In high frequency

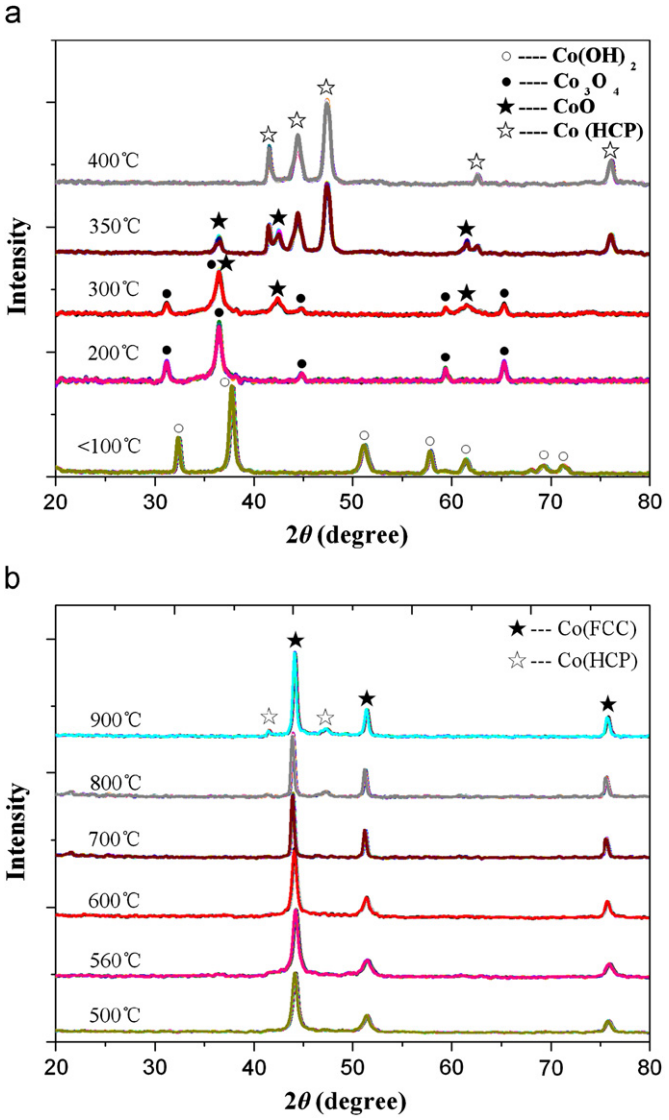

Fig. 4. XRD patterns of $Co_8/(SiO_2)_{92}$ nanocomposite powders synthesized by H_2 reduction at different temperatures for 2 h.

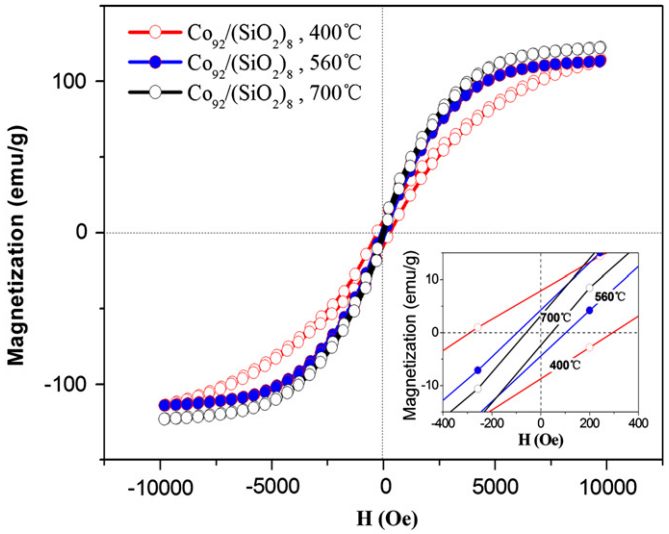

Fig. 5. Magnetic hysteresis loops for $Co_{92}/(SiO_2)_8$ NPs synthesized by H_2 reduction at 400, 560 and 700 °C, respectively.

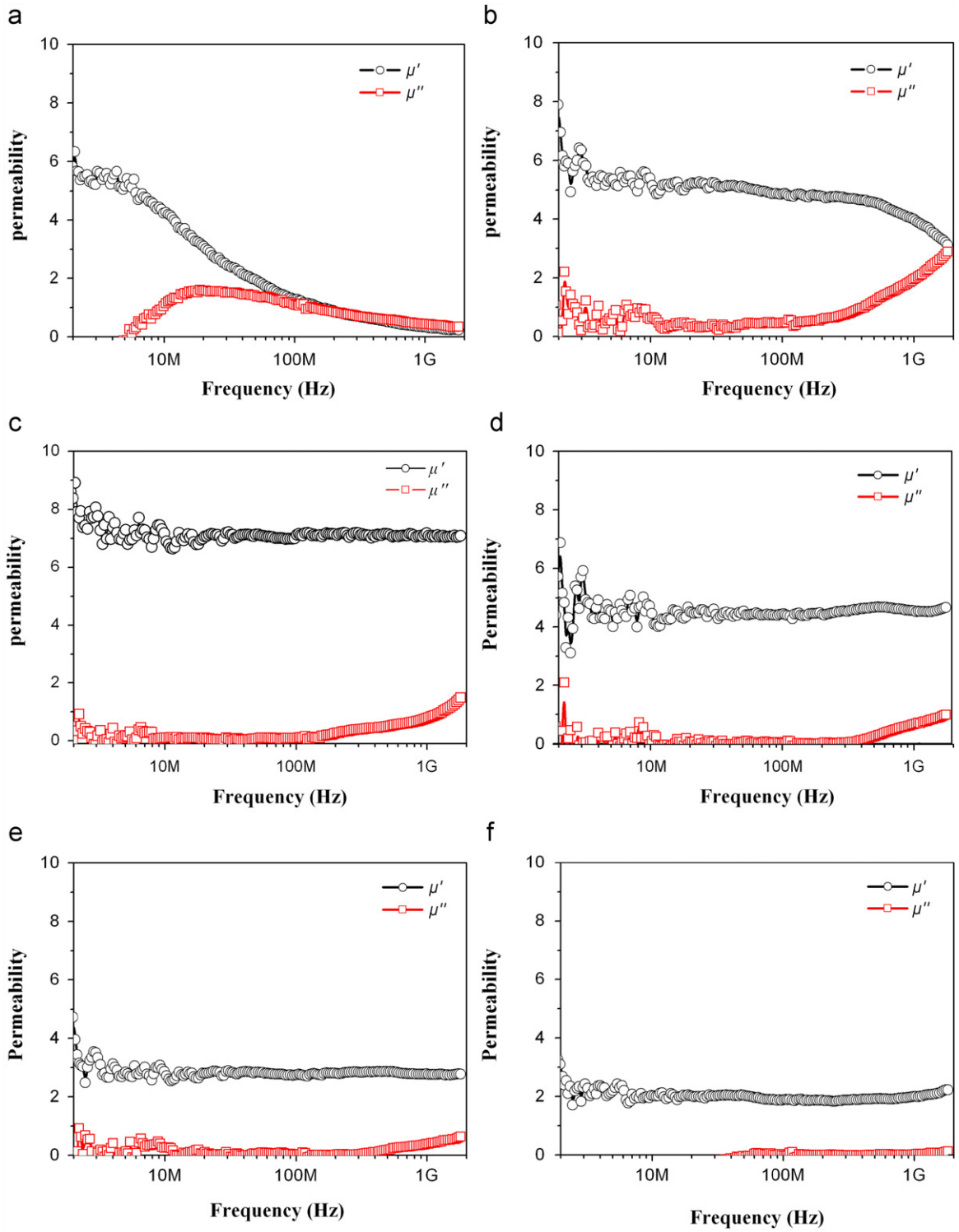

Fig. 6. Frequency dependence of complex permeability of Co/SiO_2 nanocomposites with different SiO_2 contents: (a) 3 wt%, (b) 5 wt%, (c) 8 wt%, (d) 12 wt%, (e) 16 wt% and (f) 20 wt%.

range, the motion of magnetization vector **M** cannot keep up with the applied field **H**, which results in μ'' occurrence. In as-prepared Co/SiO_2 nanocomposites, however, the size of Co is small enough that only single domain exists in the particle, so there is only a reversible rotational magnetization process when a weak magnetic field is applied to the sample. It is believed that the reversible rotation of the magnetization vector is another reason making the permeability constant in high frequency range. In addition, the size of Co NPs is much smaller than skin depth δ at 1 GHz, so eddy current induced by particle itself may be neglected.

The permeability enhancement can be attributed to the magnetic coupling between FCC-Co NPs. This magnetic coupling, which can be induced through direct exchange coupling and dipolar interaction, overcomes the inner-demagnetization effects of the particles and decreases the effective anisotropy fields of the nanocomposites, resulting in significant enhancement of

permeability value. With the further increase of SiO_2, the magnetic coupling between nanoparticles becomes weak and permeability decreases accordingly.

4. Conclusions

Co/SiO_2 nanocomposites with average Co particle size about 20–30 nm are obtained through chemical precipitation combined H_2 reducing method. Co NPs are effectively imbedded in amorphous SiO_2 mediated by Si–O–Co bonds. The particle size and crystal structure of Co are determined by reducing time, reducing temperature and SiO_2 contents. FCC-Co can be retained even when the particle size is as large as 60–80 nm. As-prepared Co/SiO_2 nanocomposites demonstrate typical soft magnetic properties with M_s as high as 125 emu/g and H_c smaller than 100 Oe. Remarkable high-frequency soft magnetic properties is obtained, in which the real part of permeability μ' (about 7) is almost independent of frequency up to 1 GHz and imaginary part μ'' is very small when the SiO_2 content is 8 wt%. This is attributed to the SiO_2 insulation and magnetic coupling between FCC-Co NPs.

Acknowledgments

This work was supported by the National Natural Science Foundation of China (No. 30772220) and Young Teacher's Supporting Foundation of Xi'an Jiaotong University (No. 08141008).

References

[1] M. Scheffler, G. Tröster, J.L. Contrras, J. Hartung, M. Menard, Microelectron. J. 17 (3) (2000) 11.
[2] Y. Zhou, Z.M. Zhou, Y. Cao, X.Y. Gao, W. Ding, J. Magn. Magn. Mater. 320 (2008) e963.
[3] L.K. Varga, J. Magn. Magn. Mater. 316 (2007) 442.
[4] K. Seemann, H. Leiste, C. Ziebert, J. Magn. Magn. Mater. 316 (2007) e879.
[5] Y.W. Zhao, T. Zhang, J.Q. Xiao, J. Appl. Phys. 93 (2003) 8014.
[6] J. Moulin, Y. Champion, L.K. Varga, J.M. Grenche, F. Mazaleyrat, IEEE Trans. Magn. 38 (2002) 3015.
[7] J.L. Snoek, Physica 14 (1948) 207.
[8] T. Nakamura, J. Appl. Phys. 88 (2000) 348.
[9] S. Sun, C.B. Murray, D. Weller, L. Folks, A. Moser, Science 287 (2000) 1989.
[10] M. Wu, Y.D. Zhang, S. Hui, T.D. Xiao, Appl. Phys. Lett. 80 (2002) 4404.
[11] K. Peng, L. Zhou, A. Hu, Y. Tang, D. Li, Mater. Chem. Phys. 111 (2008) 34.
[12] Y.D. Zhang, S.H. Wang, D.T. Xiao, J.I. Budnick, W.A. Hines, IEEE Trans. Magn. 37 (2001) 2275.
[13] N.J. Tang, W. Zhong, W. Liu, H.Y. Jiang, X.L. Wu, Y.W. Du, Nanotechnology 15 (2004) 1756.
[14] Y.W. Zhao, C.Y. Ni, D. Kruczynski, X.K. Zhang, J.Q. Xiao, J. Phys. Chem. B 108 (2004) 3691.
[15] M. Wu, Y.D. Zhang, S. Hui, T.D. Xiao, J. Appl. Phys. 92 (2002) 491.
[16] J.P. Chen, C.M. Sorensen, K.J. Klabunde, G.C. Hadjipanayis, Phys. Rev. B 51 (1995) 11527.
[17] H. Sato, O. Kitakami, T. Sakurai, Y. Shimada, Y. Otani, K. Fukamichi, J. Appl. Phys. 81 (1997) 1858.
[18] M. Erbudak, E. Wetli, M. Hochstrasser, D. Pescia, D.D. Vvedensky, Phys. Rev. Lett. 79 (1997) 1893.
[19] X. Lu, G. Liang, Z. Sun, W. Zhang, Mater. Sci. Eng. B 117 (2005) 147–152.
[20] R.C. Pedroza, S.W. da Silva, M.A.G. Soler, P.P.C. Sartoratto, D.R. Rezende, P.C. Morais, J. Magn. Magn. Mater. 289 (2005) 139.
[21] S. Ram, Mater. Sci. Eng. A 304 (2001) 923.
[22] O. Kitakami, H. Sato, Y. Shimada, Phys. Rev. B 56 (1997) 13849.
[23] S. Ram, Acta Mater. 49 (2001) 2297.